A Diffeomorphic Framework for Surrogate-based Motion Estimation in Radiation Therapy: Concept and First Evaluation

René Werner, Jan Ehrhardt, Alexander Schmidt-Richberg,
Matthias Wilms, Maximilian Blendowski, Heinz Handels

Institute of Medical Informatics
University of Lübeck
Ratzeburger Allee 160
23538 Lübeck
werner@imi.uni-luebeck.de

Abstract: Respiratory motion is a major obstacle in radiation therapy of thoracic and abdominal tumors. Techniques to cope with it such as gating and tracking techniques are based on the use of breathing signals that can be acquired easily and in real-time. These signals represent only surrogates of the motion of the inner organs and tumors. Consequently, methods are needed to estimate respiratory motion patterns of the internal structures based on surrogate measurements.
In this contribution, a diffeomorphic framework based on a multi-linear regression and the Log-Euclidean framework recently introduced in the context of diffeomorphic registration is proposed to establish such a correspondence model. The feasibility of the approach is demonstrated by means of a leave-out evaluation using 4D CT image sequences of ten lung tumor patients and simulating three different types of breathing signals: spirometry records, tracking motion of points on the diaphragm, and assessing the raising/lifting of chest wall points.

1 Introduction

Advances in imaging technologies have opened up new possibilities for diagnosis, treatment planning and image-guided therapy, with radiation therapy (RT) being a typical example. Modern image acquisition techniques and resulting images allow the RT-physicists/-physicians to accurately delineate tumors and organs at risk (OAR), to optimize treatment plans and dose distributions, to compensate for set-up errors etc.. However, in the thorax and abdomen respiratory motion still remains a limiting factor. Current 4D(=3D+t) imaging techniques like 4D CT or 4D MRI provide insights into the breathing dynamics of the individual patient, but are grounded on the application of sophisticated reconstruction techniques and are consequently not real-time capable as it would be required for image-based guidance purposes during treatment [LCC$^+$08, KMB$^+$06]. Approaches to cope with respiratory motion during irradiation – such as gated RT or tumor tracking techniques – are therefore usually steered by (mainly external) breathing signals acting as surrogates of

internal motion of tumors and OAR [KMB+06].
While it appears to be natural that a correlation exists between external breathing signals and internal respiratory motion patterns, the determination of an exact relationship is a challenging problem, especially when considering factors such as inter-cycle motion variability or phase shifts between movements of different anatomical structures. Thereby and further taking into account the complex 3D-nature of internal motion patterns, the reliability of simple 1D-surrogates like, e. g., measurements using abdominal belts is considered to be problematic, and a trend toward the use of more-dimensional surrogates can be observed [SPH08]. To efficiently use them in clinical practice, appropriate correspondence models between the surrogate signals and internal motion patterns have to be developed and evaluated.
Placed in that context, in this contribution we present a framework for establishing correspondence between motion patterns of internal structures and surrogate data based on a multi-variate multi-linear regression (MLR); therein, the internal motion patterns are derived from 4D CT images of lung tumor patients by non-linear registration [WESR+10]. In contrast to existing MLR-based models like in [ZHL+10], we embed the modeling approach within a diffeomorphic setting exploiting the Log-Euclidean framework proposed by Arsigny *et al.* [ACPA06], which in recent years has been proven to be a computationally efficient way for performing statistics on diffeomorphisms [EWSRH11]. Further, we present a first evaluation of the framework considering three different types of breathing signals: spirometry records, tracking motion of points on the diaphragm, and imitating a range imaging device (point/line laser) by evaluating raising/lifting of chest wall points.

2 Materials and Methods

The study is grounded on 4D CT data sets $\left(I_j\right)_{j\in\{1,\ldots,n_{ph}\}}$, $I_j : \Omega \subset \mathbb{R}^3 \to \mathbb{R}$ of 10 lung tumor patients. Each image sequence consists of 3D CT images of between 10 and 14 breathing phases j and features a spatial resolution of originally approx. $1\times1\times1.5$ mm^3; due to memory and computation time restrictions, the 3D images I_j were downsampled to an isotropic resolution of $1.5\times1.5\times1.5$ mm^3.
Now, for establishing the sought patient-specific correspondence models, in a first step the admissible input data of the model / for model generation has to be defined. In our case, one kind of input data is represented by the surrogate data, assumed to be described by

$$\xi : [t_0, t_{\text{end}}] \to \mathbb{R}^{n_{\text{sur}}};$$

the measurements corresponding to the acquisition times of the CT images I_j are subsequently denoted as ξ_j and the specific types of surrogate signals considered for evaluation purposes are later detailed in section 2.3. As we finally intend to derive an estimate of motion patterns of internal structures from the surrogate data, we also have – as a second kind of input data as well as the output data format of the model – to determine an appropriate representation of the internal motion. Dealing with respiratory motion and, consequently, complex deformations, we have chosen to decode internal motion in a general way by using dense displacement fields. Therefore, we assume w. l. o. g. the 3D CT volume I_1

to be the reference representation of the patient's anatomy being acquired at the phase of end-inspiration (EI). Then, internal motion is described by fields

$$u : [t_0, t_{\text{end}}] \times \Omega \to \mathbb{R}^3;$$

thus, for a voxel $x \in \Omega$ and the corresponding anatomical point, respectively, the vector $u(t, x) =: u_t(x)$ represents the displacement of the point with regard to its position in I_1. Similar to the surrogate data the displacement fields representing the motion between I_1 and the other breathing phases j and 3D images of the 4D image sequence $\left(I_j\right)_{j\in\{1,\ldots,n_{ph}\}}$ are subsequently denoted as $\left(u_j\right)_{j\in\{1,\ldots,n_{ph}\}}$ with $u_1(x) = 0$ for all $x \in \Omega$.
In the fashion of a multi-linear regression the u_j are assumed to be known and serve – together with the corresponding surrogate measurements $\left(\xi_j\right)_{j\in\{1,\ldots,n_{ph}\}}$ – as inputs of the model training phase: They form the basis of the estimation of the relationship between the surrogate data and internal motion patterns. Aiming at diffeomorphic motion estimation, which can be considered as a "natural choice in the study of anatomy as connected sets remain connected, disjoint sets remain disjoint, smoothness of anatomical features [...] is preserved, and coordinates are transformed consistently." [BMTY05], we apply a diffeomorphic registration scheme to derive the fields u_j from the 4D image sequences. The underlying theory is detailed in section 2.1. The formation of the MLR correspondence model itself and its application for estimation of internal motion patterns are explained in section 2.2.

2.1 Estimation of Internal Motion by Diffeomorphic Registration

Diffeomorphic transformations are globally one-to-one and differentiable mappings with a differentiable inverse [EWSRH11]. They can be modeled as arising from an evolution equation over unit time $t \in [0, 1]$,

$$\frac{\partial}{\partial t}\phi_t(x) = v(\phi_t(x), t) \quad \text{with} \quad \phi_0(x) = x. \tag{1}$$

Thus, for a sufficiently smooth time-dependent velocity field $v : \Omega \times [0, 1] \to \mathbb{R}^3$ parameterizing the flow $\phi : \Omega \times [0, 1] \to \Omega$, a diffeomorphic transformation $\varphi : \Omega \to \Omega$ can be computed by

$$\varphi(x) = \phi_1(x) = \phi_0(x, 0) + \int_0^1 v(\phi_t(x), t)\, dt \tag{2}$$

[DGM98, Tro98]. While the time dependence of the velocity field allows for a physically plausible interpretation, it leads to time and memory consuming algorithms if considered for image registration purposes [BMTY05, Her08]. Thus, in recent works the restriction to stationary velocity fields is examined [ACPA06, Ash07, EWSRH11]. In order to define an efficient algorithm for the time integration in (2), in the case of stationary velocity fields it can further be exploited that the set of diffeomorphisms Diff(Ω) can be seen as a differentiable manifold, and $(\text{Diff}(\Omega), \circ)$ therefore features, in addition to its general group structure, a Lie group structure with a Lie algebra $\mathfrak{g}$. Now, for a diffeomorphism

parameterized by a stationary velocity field, the velocity field is part of the tangential space $\mathcal{T}_{\text{id}}\text{Diff}(\Omega)$ at the neutral element of Diff(Ω), i. e. the vector space underlying the $\mathfrak{g}$ [Ars06]. Since Lie algebra and Lie group are connected by the group exponential map

$$\exp : \mathcal{T}_{\text{id}}\text{Diff}(\Omega) \rightarrow \text{Diff}(\Omega), \exp(tv) = \phi_t,$$

the transformation of (2) can consequently be described by

$$\varphi(x) = \phi_1(x) = \exp(v(x)), \tag{3}$$

where the velocity field v is called the (group-)logarithm of φ, $v = \log \varphi$.
In the context of Lie group theory it can further be shown that for each $v \in \mathcal{T}_{\text{id}}\text{Diff}(\Omega)$ the corresponding paths $\phi_t = \exp(tv)$ are so-called one parameter subgroups of Diff(Ω). This means especially that $\phi_s \circ \phi_t = \phi_{s+t} = \exp((s+t)v)$ for scalars s, t, and eventually

$$\exp(v) = \left(\exp\left(\frac{1}{2^N}v\right)\right)^{2^N}. \tag{4}$$

Thus, under the assumption that $\exp\left(v(x)/2^N\right) \approx x + v(x)/2^N$ for a sufficiently large N, the time integration of (2) can be substituted/executed by a recursive N-times "squaring" (self-composing) of $\exp\left(v/2^N\right)$; this represents the so-called scaling-and-squaring algorithm [ACPA06, BZO08].
Being interested in the motion fields u_j to train the sought MLR model, (3) is now employed to define a partial differential equation-driven non-linear diffeomorphic framework. Let therefore I_1 serve as reference image and the remaining 3D volumes I_j be the target images, then for each phase $j \in \{2, \ldots, n_{\text{ph}}\}$ we are searching for a transformation $\varphi_j = \text{id} + u_j$ parameterized by a stationary velocity field v_j by $\varphi_j = \exp(v_j)$ that minimizes an energy functional

$$\mathcal{J}[v_j] = \mathcal{D}[I_1, I_j \circ \varphi_j] + \alpha \mathcal{S}[v_j]. \tag{5}$$

Instead of defining an explicit image distance measure $\mathcal{D}$, however, we applied active Thirion forces. Referring to the Euler-Lagrange equations corresponding to (5), these can be interpreted as a variant of the force term related to the commonly used Sum-of-Squared Differences (SSD) measure. As the regularization term we chose a diffusion approach, $\mathcal{S}[v] = \int_\Omega \sum_{l=1}^{3} \|v_j\|^2 dx$; implementation details for the applied registration scheme can be found in [SREWH10].

2.2 Definition of the Diffeomorphic MLR Correspondence Model

Training phase: Now assuming the motion fields $\left(u_j\right)_{j\in\{1,\ldots,n_{ph}\}}$ and surrogate signals $\left(\xi_j\right)_{j\in\{1,\ldots,n_{ph}\}}$ corresponding to a 4D CT image sequence $\left(I_j\right)_{j\in\{1,\ldots,n_{ph}\}}$ to be known, the idea underlying the definition of a diffeomorphic MLR correspondence model is to work on the Log-Euclidean parametrization of the motion fields, $v_j = \log(\text{id} + u_j)$, instead of the motion fields directly. Appropriate methods to compute the logarithms

and velocity fields, respectively, for diffeomorphic transformations are proposed in, e. g., [BG08]; in the current contribution, however, explicit computation of the logarithms is not necessary because the velocity fields are given as output of the diffeomorphic registration scheme.
Now, in the context of multivariate statistics, the velocity fields v_j and the surrogate signals ξ_j are interpreted as random variables $\mathbf{V}_j$ and $\mathbf{Z}_j$, for which the motion information is described in a single column vector (i. e. $V_j \in \mathbb{R}^m$ with $m = 3n_1n_2n_3$ and n_i being the image dimension along the i-th image axis; $\mathbf{Z}_j \equiv \xi_j$). Then, a multi-variate multi-linear regression can be formulated to estimate the relationship between the matrices $\mathbf{V} := \left(\mathbf{V}_1^c, \ldots, \mathbf{V}_{n_{\text{ph}}}^c\right)$ and $\mathbf{Z} := \left(\mathbf{Z}_1^c, \ldots, \mathbf{Z}_{n_{\text{ph}}}^c\right)$, holding the centered variables $\mathbf{V}_j^c = \mathbf{V}_j - \bar{\mathbf{V}}$ with $\bar{\mathbf{V}} = \frac{1}{n_{\text{ph}}} \sum_{j=1}^{n_{\text{ph}}} \mathbf{V}_j$ and analogously $\mathbf{Z}_j^c$, such that

$$\mathbf{V} = \mathbf{B}\mathbf{Z} \tag{6}$$

with

$$\mathbf{B} = \arg\min_{\mathbf{B}'} \operatorname{tr}\left[\left(\mathbf{V} - \mathbf{B}'\mathbf{Z}\right)\left(\mathbf{V} - \mathbf{B}'\mathbf{Z}\right)^T\right] = \mathbf{V}\mathbf{Z}^T\left(\mathbf{Z}\mathbf{Z}^T\right)^{-1} = \mathbf{\Sigma}_{\mathbf{VZ}}\mathbf{\Sigma}_{\mathbf{Z}}^{-1}. \tag{7}$$

$\mathbf{\Sigma}_{\mathbf{Z}}$ is the covariance matrix of the surrogate signal observations $\mathbf{Z}$ and $\mathbf{\Sigma}_{\mathbf{VZ}}$ denotes the cross-covariance matrix of $\mathbf{V}$ and $\mathbf{Z}$. Thus, $\mathbf{B}$ represents an ordinary least squares (OLS) estimator of the relationship between the surrogate signal observations, interpreted in an MLR sense as the regressor, and the image-based estimated velocity fields, which are considered to be the regressand.
Referring to (7), it has to be noted that for more-dimensional breathing signals it is very likely that the information contributed by the different signal dimensions are highly correlated. This poses the problem of multi-collinearities, which in the perfect case leads to a singular covariance matrix $\mathbf{\Sigma}_{\mathbf{Z}}$. To avoid singularity of the matrix we introduce a Tikhonov regularization, i. e. we approximate $\mathbf{\Sigma}_{\mathbf{Z}}$ by $\mathbf{\Sigma}_{\mathbf{Z}} + \gamma\mathbf{1}$ with γ as a small positive constant [KLO09].

Motion estimation: With the computed OLS estimator $\mathbf{B}$, for any measurement $\xi(t) \equiv \mathbf{Z}(t)$, $t \in [t_0, t_{\text{end}}]$, a corresponding velocity field $\hat{v}(t)$ can be derived by

$$\hat{\mathbf{V}}(t) = \bar{\mathbf{V}} + \mathbf{B}\left(\mathbf{Z}(t) - \bar{\mathbf{Z}}\right) \tag{8}$$

and subsequently resorting the entries of $\hat{\mathbf{V}}(t)$ appropriately into the field $\hat{v}(t)$. Again exploiting (3), the associated diffeomorphic transformation can finally be derived by $\hat{\varphi}(t) = \exp(\hat{v}(t))$ and the sought motion field is given by $\hat{u}(t) = \exp(\hat{v}(t)) - \text{id}$.

2.3 Considered Types of Surrogates

The MLR framework as described above can be applied by using in principle arbitrary breathing signals. As already mentioned in section 1, in this paper we consider three different types of surrogates for a first evaluation of the framework:

Spirometry records: The reconstruction process of the 4D CT image sequences considered was based on spirometry measurements [EWS+07]. These were now used as an example of an one-dimensional surrogate, $\xi^{\text{spiro}} : t \mapsto \xi^{\text{spiro}}(t) \in \mathbb{R}$.

Tracking motion of points on the diaphragm: For a first demonstration of the potential of the multi-variate character of the correspondence model, we tracked points $x^{\text{dia}} \in \Omega$ on the diaphragm within the patients' 4D CT image sequences and interpreted the corresponding displacements $\left\{u_1\left(x^{\text{dia}}\right), \ldots, u_{n_{\text{ph}}}\left(x^{\text{dia}}\right)\right\}$ as regressor measurements. The motivation of this approach is that, on the one hand, the diaphragm can be considered as the main motor of breathing motion. On the other hand, the diaphragm is clearly visible in most medical imaging devices [KLO09] including, e. g., fluoroscopy. Tracking of diaphragm motion therefore offers the potential to serve as a real-time image-based surrogate. In a first run of the experiments, we identified and used solely the dome of the left and the right hemi-diaphragm (thus, $\xi^{\text{dia 1}} : t \mapsto \xi^{\text{dia 1}}(t) \in \mathbb{R}^{2\cdot 3}$). In the second run, additional 28 points on three concentric circles around the dome are tracked for each hemi-diaphragm (i. e. $\xi^{\text{dia 2}} : t \mapsto \xi^{\text{dia 2}}(t) \in \mathbb{R}^{2\cdot 29\cdot 3}$).

Simulating range imaging (RI) devices: As a third surrogate type we simulated the use of a point- and a line-laser for tracking lifting/raising of the chest wall based on the patient's 4D CT image sequences; point- and line-lasers can be considered as typical examples of range imaging devices in RT. For a point-laser and each breathing phase j, a ray originating from a given position above the patient is traced until it intersects with the chest wall (ray direction: anterior-posterior; air-to-soft tissue threshold: -100 HU; intersection determined with subvoxel-accuracy); for a line-laser, this procedure is repeated for a series of points on the line (line orientation: superior-inferior; line points distance = voxel spacing; scanning range $\approx$ 20 cm). Simulating the point laser, in a first run the ray origin is placed over the sternum (i. e. a standard position for RI-based gating devices; $\xi^{\text{RI, sternum}} : t \mapsto \xi^{\text{RI, sternum}}(t) \in \mathbb{R}$); the corresponding modeling accuracy is compared to an MLR-based motion detection based on ten laser positions that – considered as individual point lasers – feature the lowest residual wrt. (7) ($\xi^{\text{RI, opt. points}} : t \mapsto \xi^{\text{RI, opt. points}}(t) \in \mathbb{R}^{10}$). Finally, results are compared to the simulated line laser positioned such that again the residual of (7) is minimal ($\xi^{\text{RI, line}} : t \mapsto \xi^{\text{RI, line}}(t) \in \mathbb{R}^{150}$).

2.4 Experiments

To evaluate the accuracy of the proposed MLR correspondence model and the appropriateness of the OLS estimator to describe the relationship between the surrogate measurements/simulations and the motion fields extracted from the 4D CT image sequences, a leave-out strategy is applied: Using all breathing phases $j \in \{1, \ldots, n_{\text{ph}}\}$ but the phase of end expiration (EE) and around EE (thus, using in total all but three phases) for training purposes, capabilities of "extrapolation" of displacements (i. e. to estimate displacement fields for surrogate measurements not contained in the signal intervals used for the OLS training) are analyzed by estimating the field u_{EE} between EI and EE based on the surrogate values at EE. Interpolation capabilities are evaluated similarly by leaving out mid-respiration phases during training of the OLS estimator and then estimating the cor-

responding fields.
As quantitative measures, the accuracy of the tumor mass center motion as estimated by the MLR approach is considered (only motion estimation between EI and EE; ground truth: manual tumor segmentations within the CT images at EE and EI). Furthermore, a target registration error (TRE) is computed based on inner lung landmark correspondences determined manually within the CT data at the different breathing phases (70 landmarks per patient and breathing phase).
Results are computed for all surrogate types and runs described above and the proposed diffeomorphic MLR framework as well as for a "standard" MLR with the regression directly performed on the fields $\left(u_j\right)_{j\in\{1,\ldots,n_{ph}\}}$ and the surrogate signals $\left(\xi_j\right)_{j\in\{1,\ldots,n_{ph}\}}$.

3 Results

The results of the leave-out tests are summarized in Tables 1 and 2. Referring to the accuracy of the different types of surrogates, no significant differences can be observed between the use of the spirometry records and tracking of diaphragm points for the extrapolation scenarios ($p>0.05$ for both tumor motion estimation and the landmark-based TRE values; paired t-test); only in the case of interpolation purposes, the more-dimensional diaphragm motion offers a slightly, but significantly higher accuracy ($p<0.01$). In comparison, tracking only a single point of the chest wall leads to a significantly decreased accuracy of the MLR models ($p<0.01$). However, using more points and eventually simulating line tracking improves the accuracy with the resulting measures being slightly lower, but in a similar order than in the case of using spirometry measurements or tracking the diaphragm (differences still significant, $p<0.01$). This demonstrates the potential of information fusion and the use of multi-variate methods for the given field of application.
The results of Tables 1 and 2 additionally show that almost no differences can be observed between the diffeomorphic MLR framework and the application of the standard MLR-based motion estimation when referring to the accuracy measures considered. The potential of the diffeomorphic framework – i. e. avoiding singularities in the estimated motion fields – becomes obvious especially in the case of extrapolation. A clinically motivated example is described in figure 1; the figure also demonstrates the importance of the choice of the number of self-compositions performed in the context of the transition between the velocity fields and the transformations and motion fields, respectively (i. e. the choice of N in the scaling-and-squaring algorithm, cf. (4)).

4 Discussion

Current techniques to cope with respiratory motion in radiation therapy of thoracic and abdominal tumors like gating or tumor tracking techniques are usually grounded on the use of breathing signals (internal motion surrogates) that can be acquired easily and fast during treatment. Taking into account a trend toward the use of more-dimensional signals

Table 1: Target registration error values computed for the diffeomorphic MLR-based estimation of inner lung motion as part of the leave-out tests (EE = end expiration, EI = end inspiration, MI = mid inspiration, ME = mid expiration), listed for the different surrogate types and contrasted to values obtained by a standard (= non-diffeomorphic) MLR-based motion estimation. Given are the mean values obtained for the ten patients considered and the corresponding standard deviations.

	Target-Registration-Error [mm]		
Approach used for Motion Estimation	**EI → EE**	**EI → MI**	**EI → ME**
No motion estimation	6.8 ± 1.8	4.9 ± 1.2	2.5 ± 0.6
Intra-patient registration	1.6 ± 0.2	1.6 ± 0.1	1.5 ± 0.2
Diffeomorphic framework:			
MLR: surrogate = spirometry, ξ^{spiro}	2.0 ± 0.3	2.0 ± 0.3	1.8 ± 0.3
MLR: surrogate = diaphragm motion, $\xi^{\text{dia 1}}$	2.1 ± 0.4	1.8 ± 0.2	1.7 ± 0.3
MLR: surrogate = diaphragm motion, $\xi^{\text{dia 2}}$	2.0 ± 0.3	1.8 ± 0.2	1.6 ± 0.2
MLR: surrogate = chest wall motion, $\xi^{\text{RI, sternum}}$	4.7 ± 1.4	2.6 ± 0.9	2.4 ± 0.7
MLR: surrogate = chest wall motion, $\xi^{\text{RI, opt. points}}$	2.7 ± 0.7	2.0 ± 0.2	2.0 ± 0.4
MLR: surrogate = chest wall motion, $\xi^{\text{RI, line}}$	2.1 ± 0.4	1.9 ± 0.2	1.8 ± 0.2
Standard framework:			
MLR: surrogate = spirometry, ξ^{spiro}	2.0 ± 0.3	2.0 ± 0.3	1.8 ± 0.3
MLR: surrogate = diaphragm motion, $\xi^{\text{dia 1}}$	2.1 ± 0.5	1.8 ± 0.2	1.7 ± 0.3
MLR: surrogate = diaphragm motion, $\xi^{\text{dia 2}}$	2.0 ± 0.3	1.8 ± 0.2	1.7 ± 0.2
MLR: surrogate = chest wall motion, $\xi^{\text{RI, sternum}}$	4.7 ± 1.4	2.6 ± 0.9	2.4 ± 0.7
MLR: surrogate = chest wall motion, $\xi^{\text{RI, opt. points}}$	2.8 ± 0.7	2.0 ± 0.2	1.9 ± 0.4
MLR: surrogate = chest wall motion, $\xi^{\text{RI, line}}$	2.0 ± 0.4	1.9 ± 0.2	1.7 ± 0.2

Table 2: Accuracy of the MLR-based estimation of tumor motion between end inspiration (EI) and end expiration (EE) as obtained during the leave-out tests and based on manual tumor segmentations in the EI and EE CT data.

Approach used for Motion Estimation	**Distance of tumor mass centers [mm]**	**Jaccard index for tumor propagation**
No motion estimation	6.9 ± 6.1	0.50 ± 0.26
Intra-patient registration	0.9 ± 0.5	0.78 ± 0.06
Diffeomorphic framework:		
MLR: surrogate = spirometry, ξ^{spiro}	1.5 ± 0.9	0.74 ± 0.10
MLR: surrogate = diaphragm motion, $\xi^{\text{dia 1}}$	1.7 ± 0.9	0.71 ± 0.11
MLR: surrogate = diaphragm motion, $\xi^{\text{dia 2}}$	1.6 ± 1.3	0.72 ± 0.14
MLR: surrogate = chest wall motion, $\xi^{\text{RI, sternum}}$	4.7 ± 4.3	0.52 ± 0.25
MLR: surrogate = chest wall motion, $\xi^{\text{RI, opt. points}}$	1.7 ± 1.3	0.70 ± 0.13
MLR: surrogate = chest wall motion, $\xi^{\text{RI, line}}$	1.4 ± 1.0	0.74 ± 0.11
Standard framework:		
MLR: surrogate = spirometry, ξ^{spiro}	1.5 ± 1.0	0.73 ± 0.11
MLR: surrogate = diaphragm motion, $\xi^{\text{dia 1}}$	1.6 ± 0.8	0.71 ± 0.10
MLR: surrogate = diaphragm motion, $\xi^{\text{dia 2}}$	1.5 ± 1.2	0.71 ± 0.12
MLR: surrogate = chest wall motion, $\xi^{\text{RI, sternum}}$	4.7 ± 4.3	0.52 ± 0.25
MLR: surrogate = chest wall motion, $\xi^{\text{RI, opt. points}}$	1.8 ± 1.3	0.70 ± 0.13
MLR: surrogate = chest wall motion, $\xi^{\text{RI, line}}$	1.4 ± 0.9	0.74 ± 0.11

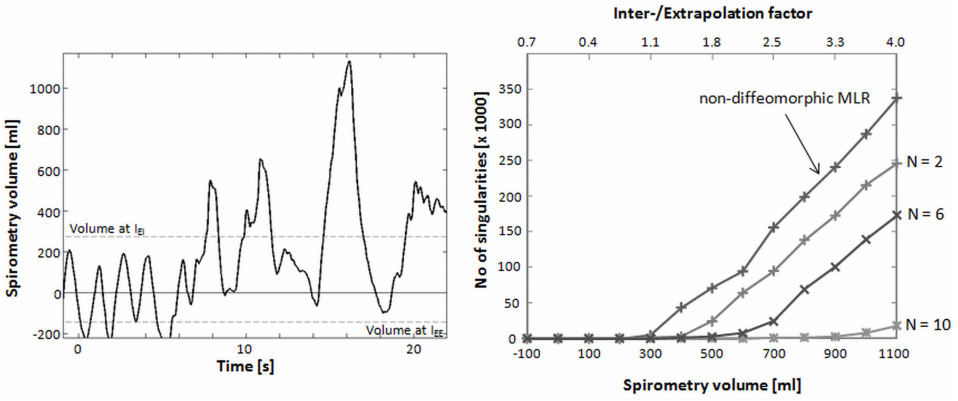

Figure 1: In the left figure, a period of the spirometry record of a lung tumor patient is shown. The zero volume indicates the measured volume for a mid-inspiration CT of the patient's 4D CT image sequence, which in the current case was chosen for treatment planning. The dashed lines represent the volumes for the 3D CT data at end inspiration (EI) and end expiration (EE). The MLR framework was applied to estimate internal motion patterns with the focus on spirometry volumes and movements not being represented as part of the 4D CT, i. e. for extrapolation purposes. In the right figure, the number of singularities in the estimated fields (voxels x with $\det\nabla\hat{\varphi}(x) < 0$) is visualized as a function of spirometry volume and the inter-/extrapolation factor; this demonstrates, on the one hand, the potential and advantage of the diffeomorphic framework proposed (please note that a factor of 1.0 means a maximum motion of ≈15 mm, while for the extreme factor of 4.0 – usually, factors of > 2 are hardly observed – maximum voxel displacements of >50 mm are computed). On the other hand, the importance of the choice of the number N of self-compositions during the scaling-and-squaring algorithm becomes also obvious.

and exploiting the Log-Euclidean framework for computing statistics on diffeomorphisms, in the current contribution we proposed a diffeomorphic MLR framework for establishing correspondence between the surrogate measurements and motion patterns of internal anatomical and pathological structures. The results demonstrate feasibility and potential of the proposed approach. In the next steps, however, thorough evaluations based on additional data sets are required; especially the use of follow-up 4D image sequences would be of interest in order to evaluate the capabilities of the OLS estimator in the presence of intra- and inter-session breathing variations.

Acknowledgments:

This study is funded in part by the German Research Foundation DFG (HA 2355/9-2).

References

[ACPA06] V. Arsigny, O. Commowick, X. Pennec, and N. Ayache. A Log-Euclidean Framework for Statistics on Diffeomorphisms. In R. Larsen et al., editors, *Medical Image Computing and Computer-Assisted Intervention, MICCAI 2006*, volume 4190 of *Lecture Notes in Computer Science*, pages 924–931. Springer, 2006.

[Ars06] V. Arsigny. *Processing Data in Lie Groups: An Algebraic Approach. Application to Non-Linear Registration and Diffusion Tensor MRI*. Thèse de sciences (phd thesis), École polytechnique, November 2006.

[Ash07] J. Ashburner. A fast diffeomorphic image registration algorithm. *Neuroimage*, 38(1):95–113, Oct 2007.

[BG08] M. N. Bossa and S. Olmos Gasso. A new algorithm for the computation of the group logarithm of diffeomorphisms. In *Workshop Proc. MICCAI 2008: MFCA 2008: International Workshop on Mathematical Foundations of Computational Anatomy.*, 2008.

[BMTY05] M. Faisal Beg, Michael I. Miller, Alain Trouvé, and Laurent Younes. Computing Large Deformation Metric Mappings via Geodesic Flows of Diffeomorphisms. *International Journal of Computer Vision*, 61(2):139–157, 2005.

[BZO08] M. Bossa, E. Zacur, and S. Olmos. Algorithms for computing the group exponential of diffeomorphisms: Performance evaluation. In *Proc. IEEE Computer Society Conf. Computer Vision and Pattern Recognition Workshops CVPRW '08*, pages 1–8, 2008.

[DGM98] P. Dupuis, U. Grenander, and M.I. Miller. Variational Problems on Flows of Diffeomorphisms for Image Matching. *Quarterly of Applied Mathematics*, LVI(4):587–600, Feb 1998.

[EWS+07] J. Ehrhardt, R. Werner, Dennis S., et al. An optical flow based method for improved reconstruction of 4D CT data sets acquired during free breathing. *Medical Physics*, 34(2):711–721, Feb 2007.

[EWSRH11] J. Ehrhardt, R. Werner, A. Schmidt-Richberg, and H. Handels. Statistical Modeling of 4D Respiratory Lung Motion Using Diffeomorphic Image Registration. *IEEE Transactions on Medical Imaging*, 30(2):251–65, Sep 2011.

[Her08] M. Hernandez. *Variational techniques with applications to segmentation and registration of medical images*. Phd-thesis, Aragon Institute on Engineering Research, University of Zaragossa, 2008.

[KLO09] T. Klinder, C. Lorenz, and J. Ostermann. Free-Breathing intra- and intersubject respiratory motion capturing, modeling, and prediction. In J.P.W. Pluim and B.M. Dawant, editors, *SPIE Medical Imaging 2009: Image Processing*, volume 7259 of *Proc. of SPIE*, pages 72590T–1–11, 2009.

[KMB+06] P. J. Keall, G.S. Mageras, J. M. Balter, et al. The management of respiratory motion in radiation oncology report of AAPM Task Group 76. *Medical Physics*, 33:3874–3900, 2006.

[LCC+08] G. Li, D. Citrin, K. Camphausen, et al. Advances in 4D medical imaging and 4D radiation therapy. *Technology in Cancer Research and Treatment*, 7(1):67–81, Feb 2008.

[SPH08] C. Schaller, J. Penne, and J. Hornegger. Time-of-flight sensor for respiratory motion gating. *Medical Physics*, 35(7):3090–3093, Jul 2008.

[SREWH10] A. Schmidt-Richberg, J. Ehrhardt, R. Werner, and H. Handels. Diffeomorphic Diffusion Registration of Lung CT Images. In B. van Ginneken, K. Murphy, T. Heimann, V. Pekar, and X. Deng, editors, *Workshop Proc. MICCAI 2010: Medical Image Analysis for the Clinic: A Grand Challenge*, pages 55–62, Bejing, China, Sep 2010.

[Tro98] Alain Trouve. Diffeomorphisms Groups and Pattern Matching in Image Analysis. *International Journal of Computer Vision*, 28(3):213–221, 1998.

[WESR+10] R. Werner, J. Ehrhardt, A. Schmidt-Richberg, A. Heiss, and H. Handels. Estimation of motion fields by non-linear registration for local lung motion analysis in 4D CT image data. *International Journal of Computer Assisted Radiology and Surgery*, 5(6):595–605, 2010.

[ZHL+10] Q. Zhang, Y.-C. Hu, F. Liu, K. Goodman, K.E. Rosenzweig, and G.S. Mageras. Correction of motion artifacts in cone-beam CT using a patient-specific respiratory motion model. *Medical Physics*, 37(6):2901–2909, Jun 2010.